Princeton Plasma Physics Laboratory

PPPL-

PPPL-

Princeton Plasma Physics Laboratory
Report Disclaimers

PPPL Report Availability

Princeton Plasma Physics Laboratory:

http://www.pppl.gov/techreports.cfm

Office of Scientific and Technical Information (OSTI):

http://www.osti.gov/bridge

Related Links:

U.S. Department of Energy

Office of Scientific and Technical Information

Fusion Links

Wave-driven countercurrent plasma centrifuge

Abraham J. Fetterman and Nathaniel J. Fisch

Department of Astrophysical Sciences, Princeton University, Princeton, New Jersey 08540, USA

(Dated: March 18, 2009)

A method for driving rotation and a countercurrent flow in a fully ionized plasma centrifuge is described. The rotation is produced by radiofrequency waves near the cyclotron resonance. The wave energy is transferred into potential energy in a manner similar to the α channeling effect. The countercurrent flow may also be driven by radiofrequency waves. By driving both the rotation and the flow pattern using waves instead of electrodes, physical and engineering issues may be avoided.

Rotating plasmas have been investigated in a variety of configurations for the separation of elements and isotopes [1–4]. Isotope separation has applications in the production of nuclear fuel [5], and in research and medical isotope production [6]. While most enriched uranium is produced by the gas centrifuge method [7], a significant number of isotopes are still produced by calutrons due to their flexibility [8].

The idea to use rotating plasma to separate isotopes was first suggested by Bonnevier, who performed one of the first experiments to test this theory [1, 9]. In preliminary experiments, significant separation was measured, but it was found that the rotation rate (and therefore separation) was limited by the Alfven critical ionization velocity at the insulator surface along the field lines [1, 10]. Further experiments revealed visocus heating fundamentally limited the separation factor in partially ionized plasmas [2].

Both of these limitations were overcome by the introduction of the vacuum-arc plasma centrifuge [3]. These pulsed devices were fully ionized, and did not have enough contact with the wall to be limited by the Alfven critical ionization velocity. However, due to their pulsed nature, throughput is limited, and the concurrent flow pattern limits the separation factor and flexibility of vacuum-arc plasma centrifuges.

The primary method for producing the radial electric field of rotating plasmas is by segmented ring electrodes at the end of the centrifuge [11]. However, the Alfven critical ionization velocity limits the speed of plasma rotation at the electrode surface, even if the plasma is fully ionized [11, 12]. The ionization and density must also be carefully controlled to maintain an electrical connection to the end electrodes [13]. Since both the product and waste exit along the field line, these electrodes will be subject to a significant particle flux. A mechanism for removing product and waste from and around the electrodes would be advantageous. It has also been found that some elements of interest, such as uranium, react strongly with electrode materials [14]. These issues suggest that an electrodeless configuration would signficantly reduce the engineering difficulty of a plasma centrifuge.

In this paper, we will describe such an electrodeless plasma centrifuge. First we will summarize advantages of the plasma centrifuge over the gas centrifuge. Next, we will give an overview of the device design and its operating parameters. Then we will describe techniques to generate the radial electric field and the countercurrent flow using radiofrequency waves.

COMPARISON WITH GAS CENTRIFUGE

The separation in a centrifuge (plasma or gas) is produced by the force balance between the pressure and centrifugal forces. Since the centrifugal force is different for each species, there will be different pressure profiles. For a constant rotation frequency Ω, the equilibrium profile is,

$$(n_2/n_1)_r = (n_2/n_1)_0 \exp\left(\Delta m\,\Omega^2 r^2/2T_i\right), \qquad (1)$$

where $\Delta m = m_2 - m_1$ is the mass difference between teh isotopes or elements being separated. In gas centrifuges, the peripheral speed is limited by the stress tolerance of the rotating shell, and so only limited values of $\alpha_0 = \exp\left(\Delta m\,\Omega^2 r^2/2T_i\right)$ can be achieved. However, in plasmas there is no such limitation.

In order to compare separation methods, we can consider three quantities to be the most important: the single stage separation factor α, the single stage separative power δU, and the energy cost per unit separative power [6]. If the fraction of the desired isotope in the waste of a separation element is x and in the product is y, the separation factor is $\alpha = y\,(1-x)\,/x\,(1-y)$. This quantity in general is independent of the concentration of the desired isotope in the feed. The separative power δU is the change in $F\phi(z)$ between the input and output streams, where F is the flow rate, $\phi(z)$ is the separative potential, $\phi(z) = (2z-1)\ln\left(z/(1-z)\right)$, and z is the concentration of the desired isotope [15].

A plasma centrifuge with length L, rotation frequency Ω, column radius a and constant temperature T has the maximum separative power, by analogy with gas centrifuges [15],

$$\delta U_{max} = 2\pi \left\langle nD_\perp \right\rangle L \left(\frac{\Delta m\Omega^2 a^2}{2T}\right)^2, \qquad (2)$$

where the average value for the density times diffusion coefficient $\langle nD_\perp \rangle$ has been used. If we assume that n is independent of radius for most of the separation region, we find $nD_\perp \approx T_i n \tau_i \kappa^2 / m_i \left(1 + \kappa\right)^2$, with τ_i being the ion collision frequency and $\kappa = 1/\left(\Omega_i \tau_i\right)$ assumed constant. If we compare this separative power with gas centrifuges, $nD_{gas} = \sqrt{T_{gas}/m}/3\sigma$, $T_{gas} = 300\,\mathrm{K}$, $\sigma \approx 5 \times 10^{-15}\mathrm{cm}^2$ [9],

$$\frac{\delta U_{plasma}}{\delta U_{gas}} \approx \frac{T_i^{1/2}}{\lambda/10} \frac{\kappa^2}{1+\kappa^2} \left(\frac{\Omega a}{10 v_a}\right)^4, \qquad (3)$$

where T_i is in eV, v_a is the peripheral speed of the gas centrifuge, and λ is the log of the Debye number.

Since the maximum v_a for gas centrifuges is around $500\,\mathrm{m/s}$, a plasma centrifuge will be comparable to a gas centrifuge in separative power if $\Omega a \approx 5\,\mathrm{km/s}$. Vacuum-arc centrifuges have achieved up to $\Omega a = 10\,\mathrm{km/s}$ for 4 cm radius columns at T_i around 1 eV [16]. Devices with large radius using Hydrogen have regularly achieved rotation speeds of 100 km/s ($T_i \sim 30$ eV [17]). In a singular case speeds of 2000 km/s were achieved ($T_i \sim 40$ keV [18]).

For our example configuration, $\Omega = 4.6 \times 10^4/\mathrm{s}$, $a = 50\,\mathrm{cm}$, $n = 10^{13}/\mathrm{cm}^3$, $T_i = 10\,\mathrm{eV}$, $L = 10\,\mathrm{m}$, the device would produce 1.6×10^{-3} mol SWU/s (separative work units/second). The estimated power usage for the waves is 57 kW, so that the total energy cost is 370 eV/SWU. This may be compared to 650 eV/SWU for gas centrifuges [5]. Although this reduction seems marginal (especially since there are certainly other loss mechanisms not accounted for), 97% of the cost of separation by gas centrifuge is due to capital costs for construction and operation [7]. In this sense, the plasma centrifuge represents a significant reduction in cost. A single gas centrifuge has a separative power of 1.2×10^{-6} mol SWU/s, so that the described plasma centrifuge may replace a cascade of 1,300 gas centrifuges.

OVERVIEW OF DESIGN

The proposed device is a multiple-mirror configuration, with at least two magnetic mirrors. An example is shown in Fig 1. The plasma is created in a central cell near the axis of the device. The ions are diffused outward radially to produce the rotation. Countercurrent flow patterns are then created in the enriching and stripping sections, with multiple mirror cells used as needed to control the flow pattern. The product stream recovering the light element is removed on the right, and the waste stream containing the heavy element is removed on the left.

In order to facilitate discussion of different parameters, and to present a unified picture of a workable device, we will use a consistent set of parameters, although different designs could vary by an order of magnitude. We consider
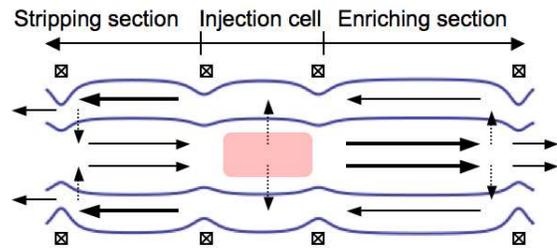

FIG. 1: An example of the countercurrent plasma centrifuge (symmetric about the center axis). The blue lines indicate field lines, the red region is where the plasma is created, the black solid arrows indicate flow patterns, and the black dashed lines indicate wave-induced diffusion.

$\Omega_i = 4.1 \times 10^4/\mathrm{s}$	$a = 50\,\mathrm{cm}$
$\tilde{\Omega}_i = 1.3 \times 10^5/\mathrm{s}$	$\rho_i = 1.5\,\mathrm{cm}$
$\Omega_E = 10^5/\mathrm{s}$	$L = 1000\,\mathrm{cm}$
$\Omega = 4.6 \times 10^4/\mathrm{s}$	$\lambda_i = 20\,\mathrm{cm}$
$\nu_i = 10^4/\mathrm{s}$	

TABLE I: Frequencies and lengths

an axial magnetic field $B = 0.1\,\mathrm{T}$, a plasma column of radius $a = 50\,\mathrm{cm}$ and length $L = 10\,\mathrm{m}$ with constant density $n = 10^{13}/\mathrm{cm}^3$ and temperature $T = 10\,\mathrm{eV}$. The electric field providing the rotation will have magnitude $E = 50\,\mathrm{V/cm}$ at $r = a$. The species we will consider separating are $^{235}\mathrm{U}$ and $^{238}\mathrm{U}$. The related frequencies and lengths are shown in Table I.

This design will describe how to create a plasma centrifuge assuming that the elements or isotopes to be separated have a similar ratio of mass to charge m/q. As such, both species will be treated as a single fluid. Once the rotation is created and flow patterns are known, the exact separation may be determined by the differential equation [19],

$$n\frac{\partial x}{\partial t} = \frac{1}{r}\frac{\partial}{\partial r}\left(nD_\perp\left[r\frac{\partial x}{\partial r} + x\left(1-x\right)\frac{\Delta m \Omega^2 r^2}{T}\right]\right) \\ - nV_z\frac{\partial x}{\partial z} + nD_\parallel\frac{\partial^2 x}{\partial z^2}. \qquad (4)$$

where x is the density fraction that is species i and $\Delta m = m_j - m_i$.

The rotation is produced by a radial current in the injection cell. The $\mathbf{J} \times \mathbf{B}$ force creates the rotation and maintains it against losses due to ion-neutral collisions. The current maintains the radial electric potential, $\Phi \approx \frac{m}{2q}\Omega_i \Omega_E r^2$, with Ω_i the cyclotron frequency and $\Omega_E = -E/rB$ the $E \times B$ rotation frequency. The true rotation frequency will differ from Ω_E due to the centrifugal force. Ignoring the diamagnetic drift, the rotation frequency is given by,

$$\Omega = \frac{\Omega_i}{2}\left(\sqrt{1 + 4\frac{\Omega_E}{\Omega_i}} - 1\right). \qquad (5)$$

In order to maximize the throughput of the device, the density must be as large as possible. The density will be proportional to the dimensionless ratio $\kappa = \nu_i/\Omega_i$. This parameter κ is limited by requirements for resonant wave-particle interactions. However, since $\lambda_i \ll L$, viscosity and angular momentum transport are strong and we will assume that the plasma is rigidly rotating (that is, the rotation frequency is independent of radius). We will also require that the stripping and enriching sections are several mean-free-paths long, so that the plasma has a local Maxwellian distribution. The length of the injection cell will be determined by requirements for the ionization of injected neutrals.

Two new technologies are involved. First, a method is described to produce the required rotation within the injection cell (rather than at end electrodes) using waves at the ion cyclotron resonance. Second, we show how a countercurrent flow pattern may be created using waves at the ion Landau resonance near a mirror boundary.

ROTATION

The use of electrodes to drive plasma rotation faces many obstacles. The Alfven critical ionization velocity must be avoided, unreactive electrode materials must be chosen to withstand extreme environments, and the plasma density and ionization must be carefully controlled to maintain electrical contact. These issues provide a strong argument for alternate methods of driving plasma rotation [14].

It was shown previously that the energy of alpha particles from fusion reactions can provide the necessary energy for plasma rotation, with the exchange mediated by appropriate radiofrequency waves [20]. It is possible to use the same technique to convert wave energy to potential energy without a kinetic energy source. This wave may be launched in the injection cell to maintain the rotation against the drag of neutrals in that chamber. If the neutral density is low in the remainder of the device, the drag in those regions will also be low.

We consider a wave that has lab frame frequency ω, parallel wave number $k_\parallel$ and poloidal mode number n_θ. The rotating frame wave frequency $\tilde{\omega} = \omega - n_\theta\Omega$ is resonant with the nth rotating frame cyclotron harmonic of a particle with parallel velocity $v_\parallel$, so that $\tilde{\omega} - k_\parallel v_\parallel = n\tilde{\Omega}_i$. We note that the rotating frame cyclotron frequency is modified by the Coriolis force, so that $\tilde{\Omega}_i = \Omega_i + 2\Omega$ [21]. Rotating frame quantities are denoted here with a tilde.

The interaction of the wave with the particle will create a correlated change in its rotating-frame perpendicular kinetic energy $\tilde{W}_\perp$ and radial position, $r\Delta r = \Delta\tilde{W}_\perp n_\theta/(m\tilde{\omega}\tilde{\Omega}_i)$ [22]. Since there is a radial electric field, the change in radial position corresponds to a change in electric potential energy, $q\Delta\Phi = -qE\Delta r = n_\theta(\Omega_E\Omega_i/\tilde{\omega}\tilde{\Omega}_i)\Delta\tilde{W}_\perp$. There is also a correlated change
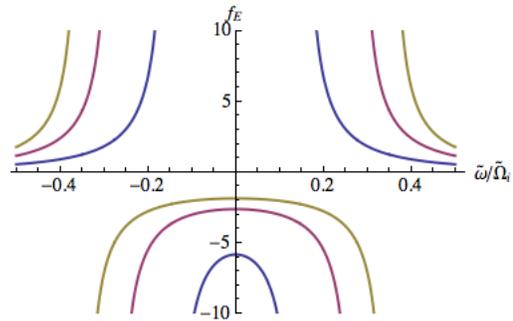

FIG. 2: The branching ratio f_E versus $\tilde{\omega}/\tilde{\Omega}_i$ for $n_\theta = -1$. Different values of $\chi = \Omega_E/\Omega_i$ are shown: $\chi = 1/4$ in blue, $\chi = 1$ in magenta and $\chi = 2.5$ in yellow.

in the parallel kinetic energy, $\Delta W_\parallel = (k_\parallel v_\parallel/n\tilde{\Omega}_c)\Delta\tilde{W}_\perp$

The fraction of the kinetic energy that is converted into potential energy was defined as the branching ratio, which is [20],

$$f_E = \frac{-n_\theta\Omega_E\Omega_i}{\omega\tilde{\Omega}_i + \tilde{\omega}k_\parallel v_\parallel/n - n_\theta\Omega_E\Omega_i}, \quad (6)$$

$$= \frac{-n_\theta\chi}{(1+4\chi)(1-\gamma+\gamma^2) + \frac{n_\theta}{4}\left(\sqrt{1+4\chi}-1\right)^2}. \quad (7)$$

where $\chi = \Omega_E/\Omega_i$ and $\gamma = \tilde{\omega}/\tilde{\Omega}_i$. For the purpose of driving rotation without a significant kinetic energy source, the potential energy must be converted from wave energy. This sets the condition $|f_E| \gg 1$. In mirrors, waves with low mode numbers n_θ have been coupled into the plasma [23–25]. Large values of $|f_E|$ are accessible for low mode numbers at low frequencies, $\tilde{\omega}/\tilde{\Omega}_i \ll 1$ (see Fig 2). Negative values of f_E correspond to the rest-frame ion energy increasing as the particle moves out radially. However, in the rotating frame the ion energy will decrease with increasing radius as long as $n_\theta/\tilde{\omega} < 0$. The reason for this discrepancy is that the wave azimuthal phase velocity $\tilde{\omega}/k_\theta$ is modified in the rest and rotating frames, while the parallel phase velocity $\tilde{\omega}/k_\parallel$ is not.

Because the collision frequency is significant, we cannot depend on phase space manipulations to result in non Maxwellian distributions lasting more than one bounce time, as was done in the case of alpha channeling. But we do, like in alpha channeling in collisionless plasmas, rely on the fact that ions will be more likely to move down density gradients in phase space. This requires that there is a limit to the motion in one direction, and that there is a density gradient along the diffusion path. The limitation in energy may be accomplished if the particle decreases in energy as it moves out ($n_\theta < 0$). Then the density must decrease fast enough as the radius increases to maintain a population inversion along the diffusion path. Assuming a constant Maxwellian temperature profile, we may
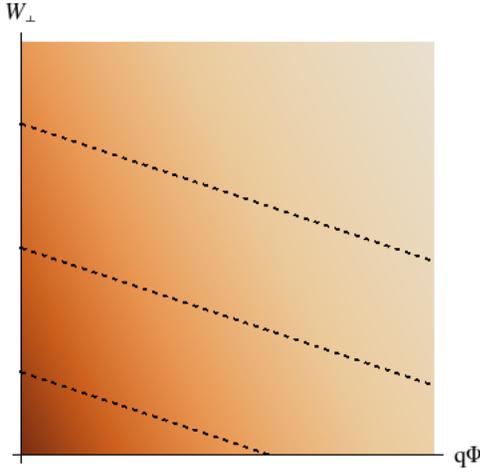
FIG. 3: Phase space density plot with diffusion paths to drive rotation drawn (dashed lines). The x axis variable is related to the radial coordinate by $q\Phi \propto r^2$. The temperature everywhere is constant.
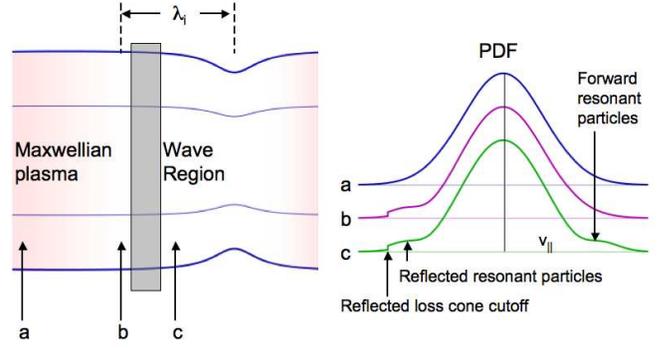

FIG. 4: Left: diagram of wave region and mirror throat. Blue lines indicate field lines. The gray boxed area is the region for wave-particle interaction. Right: particle distribution functions at locations a, b, and c on the left diagram.

write this condition,

$$0 > \Delta\left(n e^{-\tilde{W}/T}\right), \tag{8}$$

$$0 > \frac{\partial n}{\partial r}\Delta r\, e^{-\tilde{W}/T} - \frac{\Delta \tilde{W}_\perp + \Delta W_\parallel}{T} n\, e^{-\tilde{W}/T}. \tag{9}$$

Using the equation for the change in parallel energy and radius, we find the condition,

$$\frac{\partial \ln n}{\partial r} < \frac{m\tilde{\omega}^2 r}{n_\theta T}. \tag{10}$$

For $n_\theta < 0$, this yields a minimum steepness for the radial density gradient. Integrating, one finds that the maximum radius of a gaussian density distribution is $r_{max} = (\tilde{\Omega}_i/\tilde{\omega})\rho_i$. Because of this, we should choose a frequency $\tilde{\omega}$ as small as possible, even if the efficiency f_E is sacrificed. Example diffusion paths are shown in Fig 3. As the ions diffuse down the density gradient, they move outward, producing a $\mathbf{J} \times \mathbf{B}$ force that sustains the plasma rotation. Most of the energy consumed in this process is provided by the wave, although some wave energy may be absorbed or provided by the ions (depending on the sign of f_E).

An upper bound for the power requirements for this wave may be found by noting that the radial potential is the source of most thermal and rotation energy. Thus, for flow rate G, the wave would require at least the power $G\Omega^2 r_0^2/4$, assuming a constant density profile from 0 to r_0 and $\frac{1}{2}m\Omega^2 r_0^2 \gg T$. If uranium is processed at 0.4 g/s, the wave producing the rotation would require 52 kW of power. This number may be reduced if rotation energy is recovered when the particle is removed, for example by using a shaped collector [26].

COUNTERCURRENT PRODUCTION

It is clear that, if possible, countercurrent operation is desirable, since the separative effect can be multiplied many times in one device. Bonnevier suggested that the parallel flow may be driven by placing a conductor along the centrifuge axis, and driving a current to create a poloidal magnetic field. A parallel velocity gradient would then be created by shear in the $B_\theta E_r/B^2$ drift [9]. This method relies on inserting a conductor into the plasma confinement region. Our method instead uses waves to provide parallel momentum to the plasma at selected radii. This momentum balances the viscous damping of the countercurrent flow pattern.

Momentum can be provided to the ions by using waves with parallel phase velocities near the thermal velocity of the ions. The resonance condition is $\tilde{\omega} - k_\parallel v_\parallel = 0$. Since for the Maxwellian particle distribution function (PDF) f, $\partial f/\partial v < 0$, more particles will be accelerated by this wave than are damped. The result is a flattening in the tail of the Maxwellian distribution (see Fig 5). This creates net *parallel force* acting on the plasma as the Maxwellian plasma passes through the wave region.

Because the plasma is collisional, this wave must be placed within an ion mean free path λ_i of the mirror point (see Fig 4). It is the reflection condition at the mirror that will create a radially varying force profile. The reflection condition is, for mirror ratio R_m,

$$W_\parallel < W_\perp(R_m - 1) + \frac{1}{2}m\Omega^2 r^2\left(1 - R_m^{-1}\right). \tag{11}$$

In the case $R_m - 1 \ll 1$, this may be written $v_\parallel < \Omega r\sqrt{1 - R_m^{-1}}$. So as the radius increases, the cutoff velocity for reflection increases linearly. It will be helpful to define a scaled radius $r' = \Omega r\sqrt{1 - R_m^{-1}}$, with units of velocity. If we suppose that there is an identical plasma on the other side of the mirror with PDF f, and the
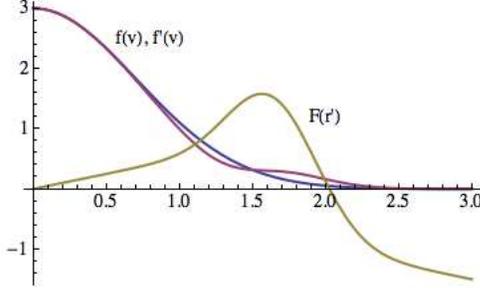
FIG. 5: The particle distribution function and parallel force. Blue is the Maxwellian PDF, while magenta is the PDF modified by a Landau resonance at $v_\parallel = 1.5\,v_{th}$, both plotted versus parallel velocity in units of v_{th}. The yellow line gives the parallel force versus radius, with radius in units of $v_{th}/\left(\Omega\sqrt{1+R_m^{-1}}\right)$. Vertical units are arbitrary.

PDF modified by the Landau resonance is f', then defining $g = f' - f$ the force produced by the wave after reflection, at scaled radius r' is,

$$F(r') = \frac{2\pi r'}{\Omega\sqrt{1-R_m^{-1}}} \int_{r'}^{\infty} g(v_\parallel)\, m v_\parallel\, v_\parallel\, dv_\parallel$$
$$- \frac{2\pi r'}{\Omega\sqrt{1-R_m^{-1}}} \int_{-\infty}^{r'} g(v_\parallel)\, m v_\parallel\, v_\parallel\, dv_\parallel. \quad (12)$$

In the integral we multiply the momentum $m v_\parallel$ by the velocity $v_\parallel$ of particles passing through the wave surface, and integrate over the PDF. The result can be seen in Fig 5. At small radii, all the resonant particles pass through the mirror, so the net force is positive. At $r' = v_{\parallel res}$, there is a maximum in the force, as particles that lost energy are reflected and particles that gained energy are transmitted through the mirror. For large radii, all resonant particles are reflected, so the net force is in the reverse direction.

We can also estimate the magnitude of this force. If we consider that N particles that are pushed an average of Δv near resonance v_{res}, such that $\partial f'(v_{res})/\partial v = 0$, we find $N = n_0 \left(v_{res}\,(\Delta v)^2\,/v_{th}^3\right) e^{-v_{res}^2/2v_{th}^2}$. These particles have parallel velocity approximately v_{res}, so the force is $F = m\Delta v\, v_{res}\, N$. At radii $|r' - v_{res}| < \Delta v/2$, the particles shifted by Δv have a net change in velocity of $2v_{res}$ since they are transmitted rather than reflected. Thus, the magnitude of the force integrated over the radius is, after some simplification,

$$F_{rf} = \pi a^2 n_0 m v_{res}^2 c_{res} \frac{(\Delta v)^3}{v_{th}^3} e^{-v_{res}^2/2v_{th}^2} \quad (13)$$

where $c_{res} = 1 + 4v_{res}^2/\left(\Omega^2 a^2(1-R_m^{-1})\right)$ is a constant taking into account the special acceleration at the resonance.

The force due to the viscosity is, for constant density and temperature [27],

$$mn_0\frac{\partial V_z}{\partial t} = 1.2\frac{n_0 T\nu_i}{\Omega_i^2}\frac{1}{r}\frac{\partial^2\,(rV_z)}{\partial r^2}. \quad (14)$$

If $V_z = V_{z0} + rV_{z1}/a$ for $r = 0$ to a,

$$mn_0\frac{\partial V_z}{\partial t} = 2.4\frac{n_0 T\nu_i}{\tilde{\Omega}_i^2}\frac{V_{z1}}{ra}, \quad (15)$$

or integrating over the volume,

$$F_{vis} = 5\pi n_0 m v_{th}^2 V_{z1}\frac{\nu_i}{\tilde{\Omega}_i^2}L. \quad (16)$$

Setting $F_{rf} = F_{vis}$ to find out the steady state V_{z1},

$$V_{z1} = v_{th}\frac{c_{res}}{5}\frac{\lambda_i}{L}\frac{a^2}{\rho_i^2}\frac{v_{res}^2}{v_{th}^2}\frac{(\Delta v)^3}{v_{th}^3}e^{-v_{res}^2/2v_{th}^2}. \quad (17)$$

We want to compare this velocity to the optimal value. The maximum for the separation fraction occurs when the total internal flux $\int_0^a |nV_z|\, r\, dr = 2\sqrt{2}\pi a n_0 v_{th}\rho_i N_f$ [19], where N_f is the flux index dependent only on the flow profile. In this case the optimum recirculating velocity is $V_{z1}^\star = 20\sqrt{2}v_{th}(\rho_i/a)N_f$. The ratio of these two quantities is,

$$\frac{V_{z1}}{V_{z1}^\star} = \frac{c_{res}}{c_{nf}}\frac{\lambda_i}{L}\frac{a^3}{\rho_i^3}\frac{v_{res}^2}{v_{th}^2}\frac{(\Delta v)^3}{v_{th}^3}e^{-v_{res}^2/2v_{th}^2}, \quad (18)$$

where we have folded $c_{nf} = 100\sqrt{2}N_f$ into one variable describing the flow shape. We can find the necessary value for the width of the resonance Δv using this equation,

$$\frac{(\Delta v)^3}{v_{th}^3} = \frac{c_{nf}}{c_{res}}\frac{V_{z1}}{V_{z1}^\star}\frac{L}{\lambda_i}\frac{\rho_i^3}{a^3}\frac{v_{th}^2}{v_{res}^2}e^{v_{res}^2/2v_{th}^2}. \quad (19)$$

We can now estimate the power used by this wave. N particles change energy by $m v_{res}\Delta v$, and they flow through the wave region with velocity v_{res}. Therefore,

$$P = \pi a^2 m n_0 v_{res}^3\frac{(\Delta v)^3}{v_{th}^3}e^{-v_{res}^2/2v_{th}^2} \quad (20)$$

$$= \pi a^2 n_0 T v_{res}\frac{c_{nf}}{c_{res}}\frac{V_{z1}}{V_{z1}^\star}\frac{L}{\lambda_i}\frac{\rho_i^3}{a^3} \quad (21)$$

Note the strong dependence on ρ_i/a, the only term that is significantly < 1, allowing cancellation of the large shape factor in c_{nf}. For the proposed configuration, (assuming $V_{z1} = V_{z1}^\star$), 5 kW of power are required for a 10 m long plasma column.

Here we have discussed waves that will drive the main countercurrent flow. Other waves may also be required to enhance radial transport near mirror boundaries other than at the injection cell (see Fig 1). This radial transport may be done using waves of the same type described in the rotation section. Waves may also be needed to enhance the removal of product or waste from the trap. Either waves described here, Alfven ion cyclotron waves [28], or other waves known to cause ion "pumpout" [29], may be used for this purpose.

CONCLUSION

We have described a countercurrent plasma centrifuge that is entirely driven by radiofrequency waves. Because the plasma is confined by the magnetic field, it is not limited in its rotation velocity. As such, much higher separation factors and separative power may be achieved than in traditional gas centrifuges.

By driving the rotation using waves, the device avoids the requirement for end electrodes to drive rotation. The end electrodes tended to incur many issues in past devices [10, 11]. They may limit the rotation speed to the Alfven critical ionization velocity. They also can react strongly with elements to be separated such as uranium [2]. Finally, they are physically in the way of removing the product and waste of the separation, and so may present many other engineering challenges.

The operation of the plasma centrifuge in a countercurrent has been suggested before [9], and equations describing the separation along the axis for a fully ionized countercurrent plasma centrifuge have been derived [19]. Countercurrent operation is critical to an efficient separation scheme, and allows an increased separation factor without multiple stages. The countercurrent is produced in the device suggested here without a center conductor. The use of waves gives precise control of the countercurrent force along the plasma axis. This will allow increased efficiency of the separation process, as the flow can be tailored to approximate an ideal cascade [5].

This theoretical work only lays the conceptual foundation for this type of device. It remains to identify waves that can be coupled into a rotating plasma and that might accomplish these effects. While low azimuthal-mode-number waves have been coupled to stationary mirrors before [23–25], not much is known about coupling waves to plasmas with supersonic rotation. In addition, a method must be found to inject neutrals into the core of the rotating plasma to be ionized, so that the density profile is peaked there. This allows the ambipolar radial diffusion to be bounded and favorable.

[1] Björn Bonnevier. Experimental evidence of element and isotope separation in a rotating plasma. *Plasma Physics*, 13:763, Sep 1971.

[2] MMB Wijnakker and EHA Granneman. Limitations on mass separation by the weakly ionized plasma centrifuge. *Z Naturfosch*, 35a:883–893, 1980.

[3] Mahadevan Krishnan, M Geva, and J. L Hirschfield. Plasma centrifuge. *Phys Rev Lett*, 46(1):36–38, Jan 1981.

[4] Tihiro Ohkawa and Robert Miller. Band gap ion mass filter. *Phys Plasmas*, 9(12):5116, Jan 2002.

[5] M Benedict. *Nuclear chemical engineering*. McGraw Hill, 1981.

[6] MW Grossman and TA Shepp. Plasma isotope-separation methods. *IEEE Transactions on Plasma Science*, 19(6):1114–1122, Jan 1991.

[7] United states gas centrifuge program for uranium enrichment. Technical report, US Department of Energy, 1977.

[8] J Tracy and J Terry. Availability of enriched isotopic materials used for accelerator targets — present and future. *Nuclear Instruments and Methods in Physics Research Section B: Beam Interactions with Materials and Atoms*, 10-11:972–975, May 1985.

[9] B Bonnevier. Diffusion due to ion-ion collisions in a multicomponent plasma. *Arkiv Fysik*, 33:255, 1967.

[10] J Bergstrom. Experiments on the velocity distribution of a rotating plasma. *Nuclear Instruments and Methods*, 133(2):347–353, Mar 1976.

[11] B Lehnert. Rotating plasmas. *Nuclear Fusion*, 11:485, 1971.

[12] H Alfvén. Collision between a nonionized gas and a magnetized plasma. *Rev. Mod. Phys.*, 32(4):710–713, Oct 1960.

[13] AA Bekhtenev and VI Volosov. Generation of a radial electric field in a rotating plasma. *Soviet Physics: Technical Physics*, 23:938–941, 1978.

[14] Erik A Witalis. Electrodeless plasma isotope centrifuge. *Atomkernenergie Kerntechnik*, 38:32, Mar 1981.

[15] K Cohen. *The theory of isotope separation as applied to the large scale production of U-235*. McGraw Hill, 1951.

[16] Mahadevan Krishnan. Centrifugal isotope separation in zirconium plasmas. *Physics of Fluids*, 26(9):2676, Jan 1983.

[17] R F Ellis, A Case, R Elton, J Ghosh, H Griem, Adil B Hassam, Robert A Lunsford, Sarah Jessica Messer, and C Teodorescu. Steady supersonically rotating plasmas in the maryland centrifugal experiment. *Physics of Plasmas*, 12:55704, 2005.

[18] GF Abdrashitov, AV Beloborodov, VI Volosov, VV Kubarev, YuS Popov, and YuN Yudin. Hot rotating plasma in the psp-2 experiment. *Nuclear Fusion*, 31:1275, 1991.

[19] AA Ivanov and NN Timchenko. Counterstreaming mass separation of ions in a fully ionized rotating plasma. *Soviet Journal of Plasma Physics*, 16:863–866, 1990.

[20] Abraham J Fetterman and Nathaniel J Fisch. alpha channeling in a rotating plasma. *Phys Rev Lett*, 101(20):205003, Nov 2008.

[21] B Bonnevier and B Lehnert. The motion of charged particles in a rotating plasma. *Arkiv for Fysik*, 16:231–236, 1960.

[22] Nathaniel J. Fisch and JM Rax. Interaction of energetic alpha particles with intense lower hybrid waves. *Phys Rev Lett*, 69:612–615, Jan 1992.

[23] Y Amagishi and M Inutake. Conversion of compressional alfvén waves into ion-cyclotron waves in inhomogeneous magnetic fields. *Phys. Rev. Lett.*, 48(17):1183–1186, Apr 1982.

[24] R Majeski, J. J Browning, S Meassick, N Hershkowitz, T Intrator, and J. R Ferron. Effect of variable eigenmode excitation on rf stabilization of a mirror plasma. *Phys Rev Lett*, 59(2):206–209, Jul 1987.

[25] Y Yamaguchi, M Ichimura, H Higaki, S Kakimoto, K Nakagome, K Nemoto, M Katano, H Nakajima, A Fukuyama, and T Cho. Eigenmode formation of icrf

waves in gamma 10. *Plasma Phys Contr F*, 48:1155, Aug 2006.

[26] AA Bekhtenev, VI Volosov, VE Bal'chikov, MS Pekker, and YuN Yardin. Problems of a thermonuclear reactor with a rotating plasma. *Nuclear Fusion*, 20:579–597, 1980.

[27] SI Braginskii. Transport processes in a plasma. *Reviews of Plasma Physics*, 1:205–311, 1965.

[28] T Goto, K Ishii, Y Goi, N Kikuno, Y Katsuki, M Yamanashi, M Nakamura, M Ichimura, T Tamano, and K Yatsu. Ion diffusion in a velocity space induced by alfvén ion cyclotron mode observed in a mirror plasma. *Phys Plasmas*, 7(6):2485, Jan 2000.

[29] D. E Baldwin. End-loss processes from mirror machines. *Rev. Mod. Phys.*, 49(2):317–339, Apr 1977.